High-resolution data-driven models of Daylight Redirection Components

Lars Oliver Grobe[1/2], Stephen Wittkopf[1], Zehra Tugce Kazanasmaz[2]

1 Competence Center Envelopes and Solar Energy, Lucerne University of Applied Sciences and Arts, Horw, Switzerland, larsoliver.grobe@hslu.ch
2 Department of Architecture, Faculty of Architecture, Izmir Institute of Technology, Urla, Turkey

Abstract

Daylight Redirecting Components (DRCs) guide daylight to zones with insufficient daylight exposure. They reduce energy demand for lighting, heating and cooling, and improve visual and thermal comfort. The data-driven model in Radiance is a means to model DRCs in daylight simulation. Rather than internal optical mechanisms, their resulting Bidirectional Scattering Distribution Function (BSDF) is replicated.

We present models of two DRCs that are generated from measurements. The impact of the following three necessary steps in the generation of data-driven models from measured BSDF shall be evaluated:
1) interpolation between measurements at sparse sets of incident directions;
2) extrapolation for directions that cannot be measured;
3) application of a directional basis of given directional resolution.

It is shown that data-driven models can provide a realistic representation of both DRCs. The sensitivity to effects from interpolation differs for the two DRCs due to the varying complexity of their BSDFs. Due to the irregularity of the measured BSDFs, extrapolation is not reliable and fails for both tested DRCs. Different measurement and modeling protocols should be applied to different class systems, rather than aiming at a common low-resolution discretization.

Keywords

daylight simulation, data-driven model, BSDF, Radiance

DOI 10.7480/jfde.2017.2.1743

1 INTRODUCTION

A Daylight Redirecting Component (DRC) controls the admission and directional distribution of daylight in buildings. The application of a DRC aims to optimize the utilization of daylight for visual and thermal comfort, well-being and energy efficiency (Gago, Muneer, Knez, & Köster, 2015; Hoffmann et al., 2016). Typical applications of DRCs include the upward deflection of daylight transmitted through the facade to achieve even illumination, or the directional selective transmission only of diffused daylight through horizontal glazing (Ruck et al., 2000; Nair, Ramamurthy, & Ganesan, 2014). Deflection and directional selectivity are some examples of the irregular optical properties of DRCs that can be utilized for optimized daylight performance, but are beyond the capabilities of typical simulation tools employed in building design (Ward & Shakespeare, 1998). To address this lack of predictability as a barrier for the widespread and successful application of the technique, different modeling approaches have been demonstrated for the application in daylight simulation.

Software algorithms such as forward ray-tracing or the bidirectional combination of backward ray-tracing and forward photon-mapping can replicate the light propagation through DRCs based on geometric models. Photon mapping has been implemented in the daylight simulation software Radiance (Noback, Grobe, & Wittkopf, 2016; Schregle, Bauer, Grobe, & Wittkopf, 2015; Schregle, Grobe, & Wittkopf, 2016) and was extended to support even advanced simulation techniques such as Climate-Based Daylight Modeling (CBDM). However, this explicit approach demands highly detailed simulation models in cases where the micro-structures in the scale of millimeters comprising DRCs covering entire building facades shall be modeled geometrically.

Models of the Bidirectional Scattering Distribution Function (BSDF) replicate the effective light scattering characteristics of DRCs rather than the comprised geometric structures causing it. Such models describe light propagation as a function of incident and outgoing light direction through a surface. The two directions, relative to a coordinate system attached to the surface of the DRC, are typically expressed as pairs of elevation and azimuth angles θ,φ. The BSDF approximates light scattering as a uniform, average property of a thin surface. Analytic models of the BSDF of the DRCs have been developed and validated (Greenup, Edmonds, & Compagnon, 2000; Maamari et al., 2006; Laouadi & Parekh, 2007). However, the development of such custom models for particular devices and applications is elaborate and has limited scope for generalization.

A general approach is the use of data-driven models of the BSDF. Such models comprise a discrete set of luminous coefficients, evaluating the light propagation through the device for incident and outgoing directions merged into regions according to a given directional basis. They can be generated by computational simulation as well as from measurements (Mohanty Yang, & Wittkopf, 2012; McNeil, Lee, & Jonsson, 2017). As a "black box", data-driven models hide the complexity of the internal optical mechanisms effecting light propagation through the device from simulations employing the model (Kuhn, Herkel, Frontini, Strachan, & Kokogiannakis, 2011; Appelfeld, McNeil, & Svendsen, 2012). A symmetric directional basis of 145 incident and 145 outgoing directions is in widespread use and supported by a set of software tools mainly developed by Lawrence Berkeley National Laboratory (LBNL), such as Radiance and Window. The latter allows the combination of the BSDFs of co-planar fenestration layers into that of an entire glazing assembly, and provides an interface for the Complex Glazing Database. The directional basis is employed in multiple domains of building simulation and backs advanced CBDM methods such as the three-phase method (Klems, 2013; McNeil & Lee, 2013). An asymmetric directional basis of 145 incident and 1297 outgoing directions was recommended by the International Energy Agency (IEA) and can be employed to pre-compute transmission through DRCs with mkillum in Radiance (de Boer, 2005; Kämpf & Scartezzini, 2011).

The highest directional resolution can be achieved by the locally adaptive tensor-tree format of Radiance, allowing up to 16,384 incident and 16,384 outgoing directions. To be applicable in simulation, and to allow sharing and re-use such as in model libraries, a compact representation for the data-driven model is required. Starting from a four-dimensional tensor of initially constant directional resolution, a data-reduction algorithm selectively merges cells representing adjacent directions with little variance in the BSDF to generate the compact tensor-tree (Ward, Mistrick, Lee, McNeil, & Jonsson, 2011; Ward, Kurt, & Boneel, 2012). The combination of the optical properties of fenestration layers described by the tensor-tree format has been demonstrated as a reflection of the method implemented in Window (Grobe, 2017).

The use of discrete data to describe the continuous BSDF introduces problems of resolution into the generation, storing and application of models. Measurements sample the BSDF for a finite set of incident and outgoing directions. This set of directions is bound to the geometric constraints of the instrument, excluding, for example, directions close to grazing and retro-reflection (Krehel, Grobe, & Wittkopf, 2017). While their underlying dataset is incomplete by necessity, models must provide coefficients for any pair of directions, and therefore rely on interpolation and extrapolation. Data-reduction such as the merging of directions leads to a loss of information in the model.

In this research, the impact of both the interpolation and extrapolation in the generation of models from measurements, and the effect of directional resolution and data-reduction applied to the data-driven model shall be assessed for two exemplary DRCs.

A better understanding of the parameters defining measurement and model generation will guide the generation and application of data-driven BSDF models. Such models would provide a general means to better predict the daylight performance of DRCs in buildings, supporting both practitioners and researchers in the field of daylighting.

2 METHODOLOGY

2.1 TWO CASES OF DAYLIGHT REDIRECTING COMPONENTS

The selected case studies focus on typical examples of shading and non-shading DRCs for applications in vertical and horizontal glazing. The examples employ the optical mechanisms of reflection and refraction on periodic structures. Due to the small size of these structures, their scattering properties are perceived as uniform when seen from the position of a typical observer. It is therefore possible to model both DRCs by their effective BSDFs rather than explicit modeling of the geometrical structures causing their irregular transmission characteristics.

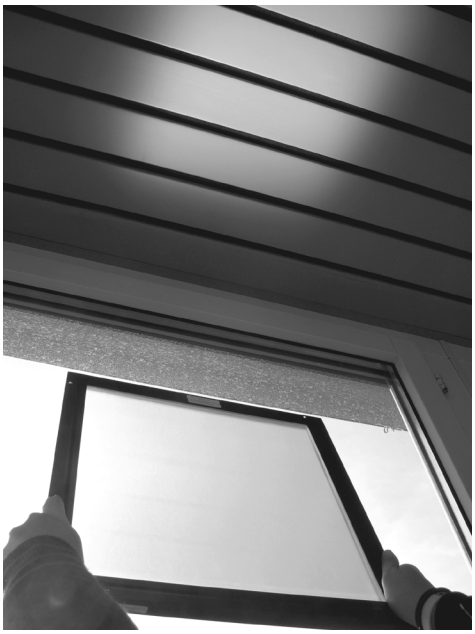

FIG. 1 DRC_1 deflecting sunlight upward

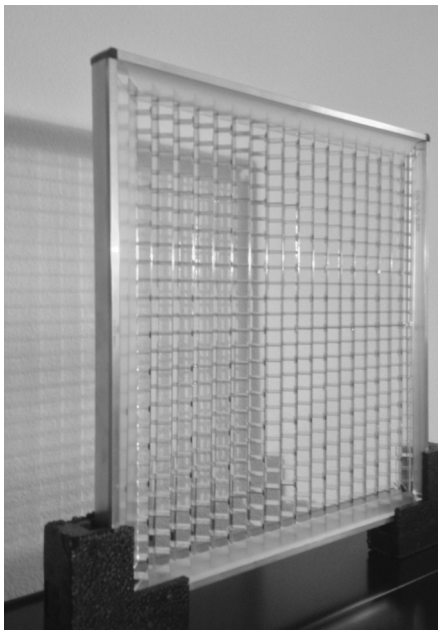

FIG. 2 DRC_2 controlling direct transmission.

DRC_1 (Fig. 1) is a glazing unit with applied films. A prismatic film is laminated on the inward-facing surface of an outer pane and deflects incident light. A diffusing film is applied to the inner pane to achieve smooth light distribution. The system improves daylight supply by deflection but provides no shading effects (Kazanasmaz, Grobe, Bauer, Krehel, & Wittkopf, 2016; McNeil et al., 2016). It can be employed e.g. in the upper zone of windows. The exact geometry of the micro-structures on both films is not known. The utilization of a data-driven model, based on measured BSDF data, allows the replication of its transmission characteristics even without detailed knowledge of the system's composition.

DRC_2 (Fig. 2), a grid of tilted anidolic light-shafts, reflects direct sunlight but transmits and evenly distributes diffuse skylight. It can control solar gains and glare when applied to skylights. The geometry of its highly reflective structure is shown in detail by Grobe et al. (2015).

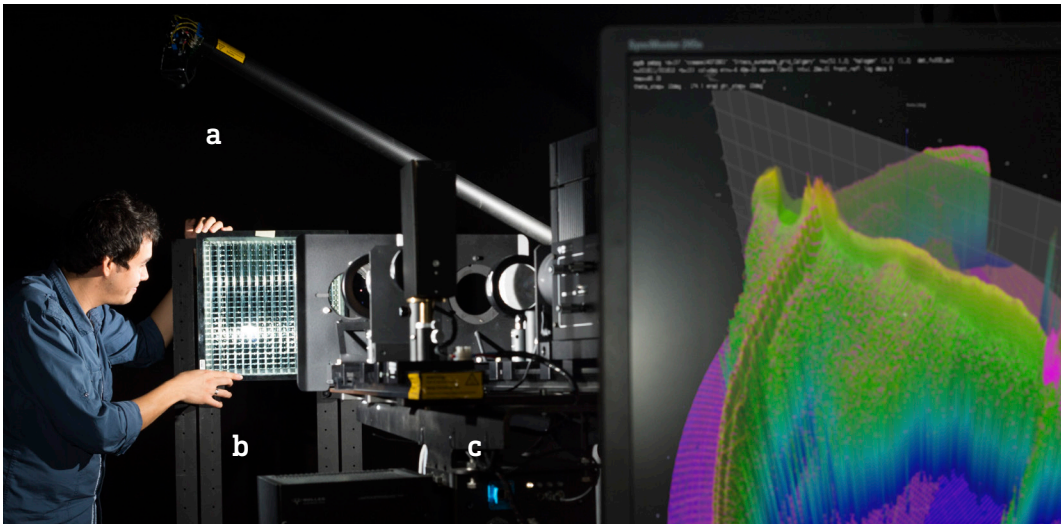

FIG. 3 Gonio-photometer, comprising detector (a) moving around rotatable sample (b), and illuminator (c).

2.2 MEASUREMENT

The BSDFs of the DRCs are measured on a scanning gonio-photometer as shown in Fig. 3.
The characterization of each DRC comprises measurements of the illuminator's intensity distribution followed by the recording of light scatter for each given incident direction. The incident direction is set by rotation of the sample, and the detector subsequently performs a continuous scan around the sampling aperture while recording illuminance E_s. The scan path is adaptive to the measurement and allows refinement e.g. for regions where transmission peaks occur.

Due to the prior beam characterization, the BSDF can be computed without photometric calibration from E_s, the power of the incident beam P_i (the integration of the unobstructed measurement) and the cosine of the outgoing elevation angle θ_s: BSDF = $E_s \times P_i^{-1} \times \cos(\theta_s)^{-1}$ (Apian-Bennewitz, 2010).

The fine structures of DRC_1 allow to focus of the illuminator on the detector for maximum directional resolution. The BSDF of DRC_2 is measured under collimated illumination, leading to a widened illuminated sampling aperture covering a representative number of periodical structures.

An asymmetric resolution of coarse incident directions θ_i,φ_i and dense outgoing scattered light directions θ_s,φ_s is chosen, assuming that features in the BSDFs require dense sampling of outgoing directions, but change only gradually between adjacent incident directions. Due to the symmetry of both DRCs, incident azimuth angles are varied as φ_i = 0° to 180°. For DRC_1, φ = 0° corresponds to up, for DRC_2 to North in typical applications.

Three sets of incident directions are distinguished (Fig. 4):

- *Coarse* (black): Low resolution with θ_i = 10° to 50° in increments of 20°, φ_i = 0° to 180° in increments of 30°.
- *Refined* (green): Refining *Coarse* with θ_i = 0° to 60° in increments of 10°, φ_i = 0° to 180° in increments of 15°.
- *High* (blue): Complementing *Coarse* and *Refined*, this dataset comprises incident elevation angles above 60°.

To test interpolation and extrapolation, the BSDFs for two additional incident directions T1 θi = 40°, φ_i = 30° and T2 θ_i = 70°, φ_i = 30° (red) are measured. In the results, these directions are shown mirrored as red circles.

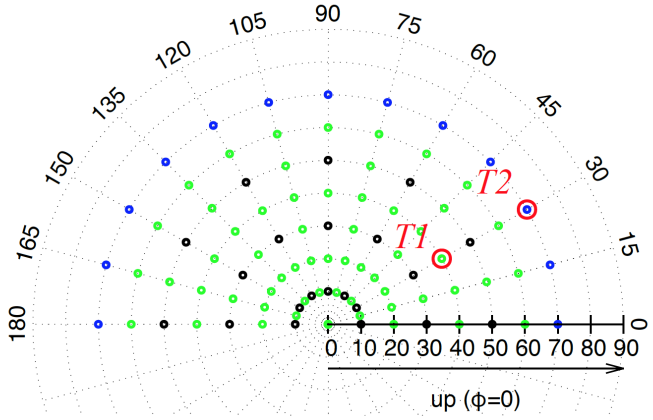

FIG. 4 Incident directions *Coarse* (black), *Refined* (green), *High* (blue),*T1* and *T2* (red).

2.3 MODEL GENERATION

Three data-driven models are generated from the three datasets. The process comprises three passes:

- *pabopto2bsdf* fits a set of radial basis functions as interpolants to the four components (reflection front/back and transmission front/back) of the measurement.
- These interpolants are subsequently sampled by the command *bsdf2ttree*[1] into a four-dimensional tensor of $2^{4\times7}$=268,435,456 elements. Higher resolutions are not possible on typical hardware due to memory constraints.
- *bsdf2ttree* internally calls rttree_reduce to reduce this vast amount of data by merging adjacent directions of low local variance until 90% of the initial dataset is eliminated, and saves the resulting tensor tree into a XML-formatted file.

The method provides a set of three BSDF-models of adaptive resolution for each DRC.

- $M1_{DRC1}$, $M1_{DRC2}$ comprise BSDF from *Coarse*.
- $M2_{DRC1}$, $M2_{DRC2}$ comprise datasets *Coarse* and *Refined*.
- $M3_{DRC1}$, $M3_{DRC2}$ comprise *Coarse*, *Refined* and *High*.

2.4 COMPARISON OF TRANSMISSION DISTRIBUTIONS

To evaluate the effect of parameters in the measurement and model-generation, pairs of the BSDF for a given direction are compared. We evaluate only transmission to the interior, which is of particular importance in building applications.

To maintain readability up to high outgoing directions, the Differential Scattering Function (DSF), equal to $BSDF(\theta_i,\varphi_i,\theta_s,\varphi_s)\cos(\theta_s)$, is plotted, rather than the BSDF. The latter, due to the division by $\cos(\theta_s)$, tends to exaggerate data at measurement points close to grazing. The transmission distributions are plotted in polar coordinates, the center being $\theta = 180°$ and $\varphi = 0°$ aiming right.

2.5 EVALUATION OF THE EFFECTS OF INTERPOLATION AND EXTRAPOLATION

The BSDFs of both DRCs for direction *T1*, as predicted by *M1* and *M2*, are compared to the measurements. Predictions by *M1* are results of interpolation, while *M2* rely on measured data.

The measured BSDFs of DRC_1 and DRC_2 for T2 are compared to the extrapolated BSDFs from *M2* and *M3*. As no data for incident directions above $\theta_i = 60°$ is employed in the generation of *M2*, these models provide results based on extrapolation. *M3* comprises measured data for the queried incident direction.

EVALUATION OF THE EFFECTS OF RESOLUTION AND DATA-REDUCTION

For both DRCs, variants of *M3* of reduced resolution (tensor of $2^{4\times6}$=16,777,216 elements representing $2^{6\times2}$ incident and $2^{6\times2}$ outgoing directions) without data-reduction are generated. These are compared to variants of high resolution ($2^{7\times2}$ incident and $2^{7\times2}$ outgoing directions), but with a data-reduction of 97% applied, leading to comparable model sizes.

3 RESULTS AND DISCUSSION

3.1 MEASUREMENT

Fig. 5 and Fig. 6 show the DSF of DRC_1 and DRC_2 measured for *T1* and *T2*. The prismatic structure of DRC_1 spreads the scattered light to a rim with an upward peak for *T1*. DRC_2 shows two forward peaks for *T1* and a pattern of scattered light on the opposite side of the φ_i = 0°,180° plane. These peaks disappear towards the *T2* direction with a remaining distribution of diffused light.

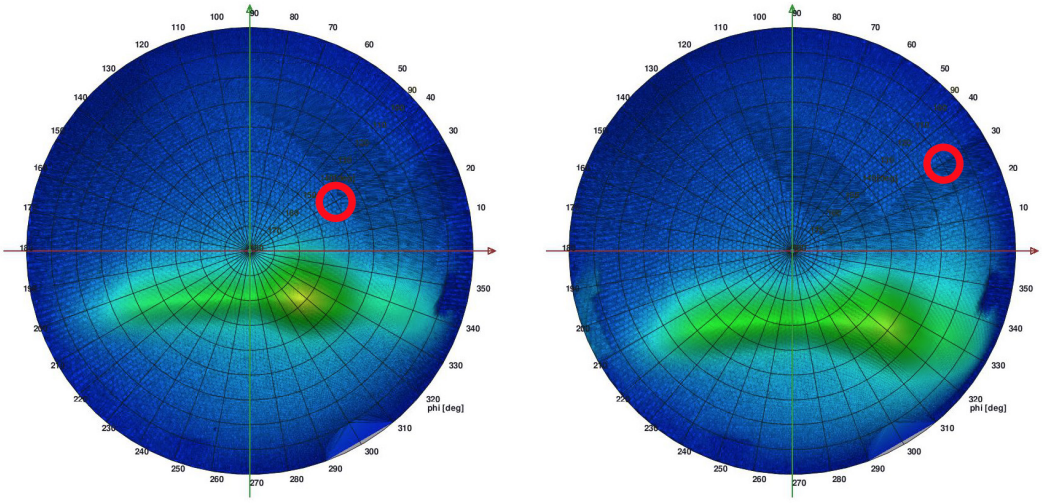

FIG. 5 Measurement: DSFs of DRC_1 for incident direction *T1* (left, red) and *T2* (right, red).

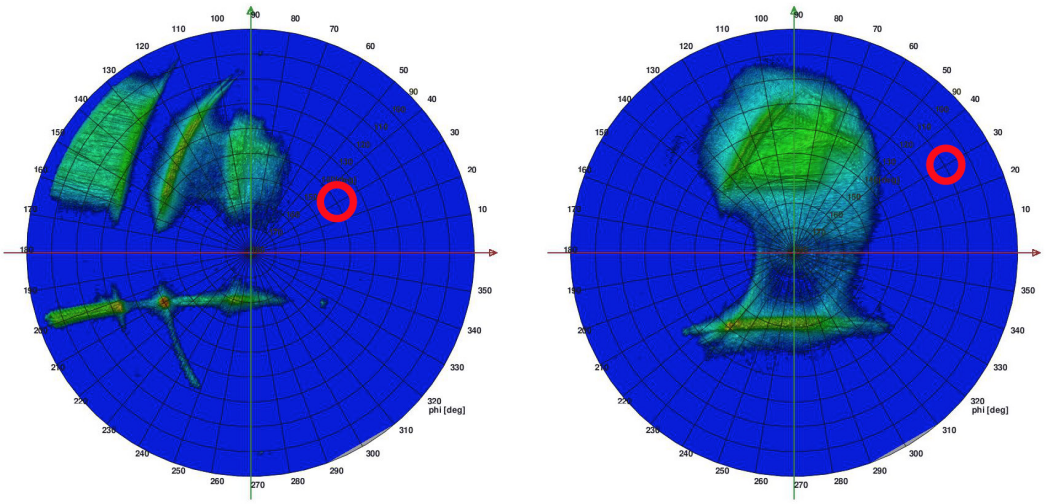

FIG. 6 Measurement: DSFs of DRC_2 for incident direction *T1* (left, red) and *T2* (right, red).

3.2 INTERPOLATION EFFECTS

M1 and *M2* lead to almost identical results for DRC_1 but do not show the ridge as pronounced measurements. Transmission to the downward direction (lower left quadrant) is underestimated by *M1* when compared to *M2* (Fig. 7).

For DRC_2, M1 replicates the configuration of features found in the measurement, such as a strong peak due to direct transmission at θ_s = 140°, φ_s = 210° (Fig. 8). The shape of other features, such as a secondary peak at θ_s = 120°, φ_s = 200° and two parallel rims in the upper half of the plot, are not maintained by *M1,* but *M2*. The latter only differs from the measurement by the less pronounced contours of its features, and a gradient toward grazing for which no measured data exists.

The interpolation by *M1* replicates the characteristic upward deflection of DRC_1 as well as the distinct features of DRC_2. The underestimation of downward transmission through DRC_1 may however effect results in daylight simulation.

3.3 EXTRAPOLATION EFFECTS

As shown in Fig. 9, the extrapolated DSF of DRC_1 for *T2* from *M2* is almost flat in the deflected upward direction and lacks any peaks, which are present in the result from *M3*. Model *M2* does not replicate the characteristic deflection of light toward the ceiling for high incident elevation directions, if these are not within the boundaries of the measurement.

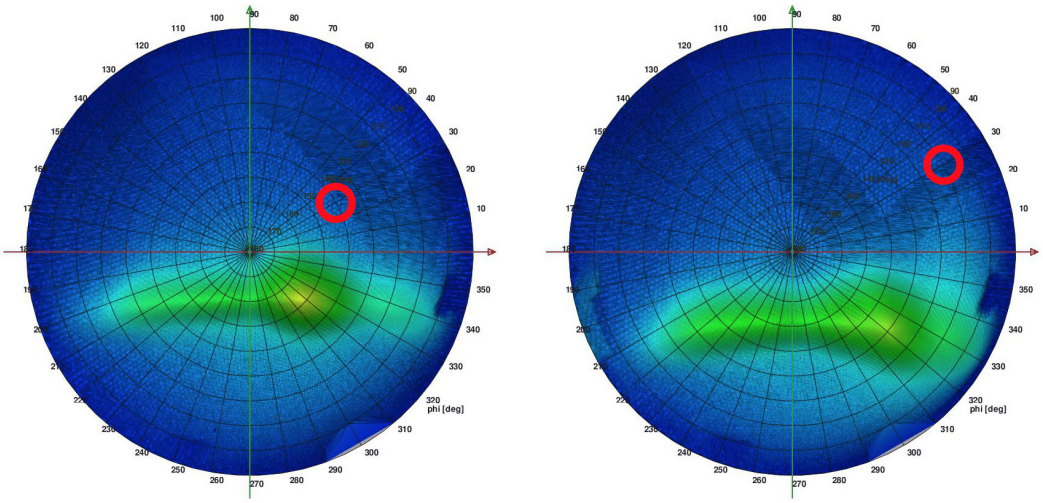

FIG. 7 Predicted DSF of DRC_1 for incident direction *T1* (red) from interpolated *M1* (left) and measured *M2* (right).

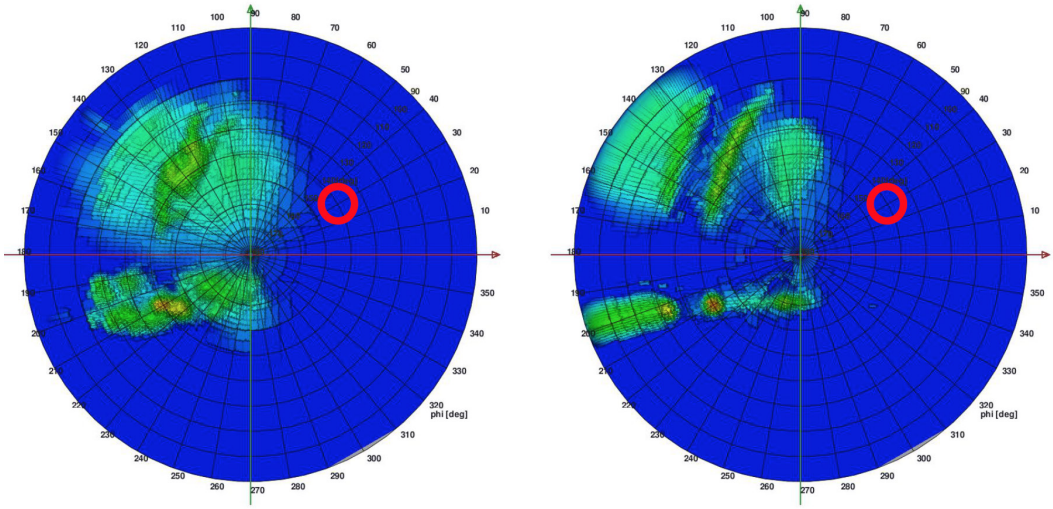

FIG. 8 Predicted DSF of DRC_2 for incident direction *T1* (red) from interpolation *M1* (left) and measurement *M2* (right).

As no diffused background is present in the DSF of DRC_2, and no peaks in the complex DFS for *T2* are extrapolated, *M2* indicates almost zero transmission. This is contradicted by *M3* (Fig. 10), which closely matches the measured distribution. Due to the typical horizontal installation of DRC_2, this corresponds to a significant underestimation of low sun angles e.g. in the morning and afternoon, if the boundaries of the measurement are not extended.

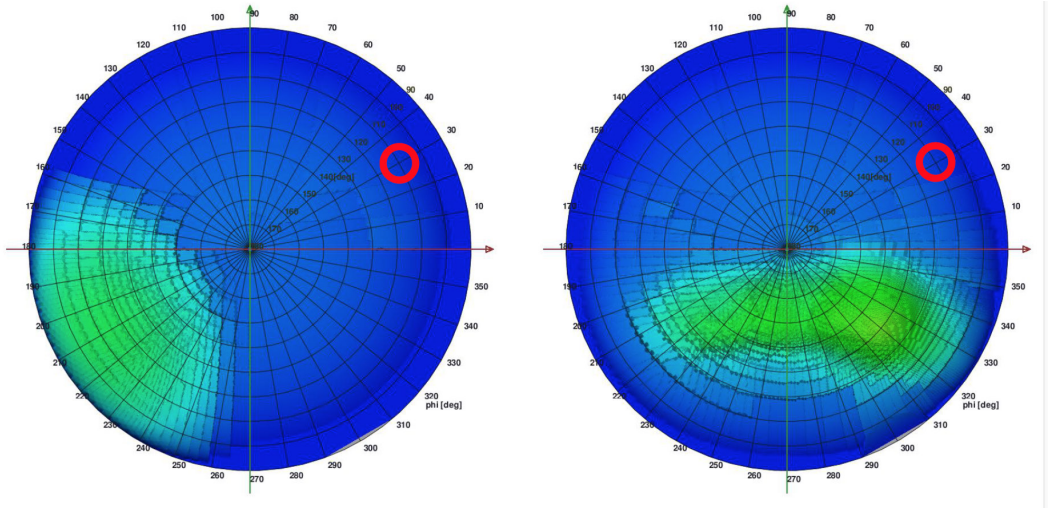

FIG. 9 Predicted DSF of DRC_1 for incident direction *T2* (red) from extrapolation *M2* (left) and measurement *M3* (right)

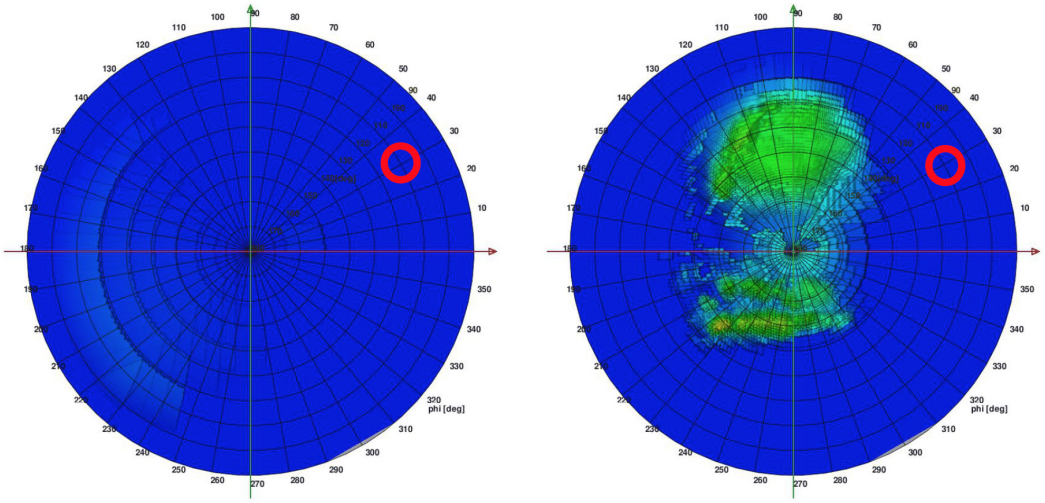

FIG. 10 Predicted DSF of DRC_2 for incident direction *T2* (red) from extrapolation *M2* (left) and measurement *M3* (right)

3.4 EFFECTS OF RESOLUTION AND DATA-REDUCTION

Fig. 11 and Fig. 12 show the DSFs for DRC_1 and DRC_2 at incident direction *T1* at resolution k = 6 without, and k = 7 with 97% data-reduction applied. While the latter can better resolve the forward peak of DRC_2 (Fig. 12, right) data-reduction does not affect any important features for the two DRCs.

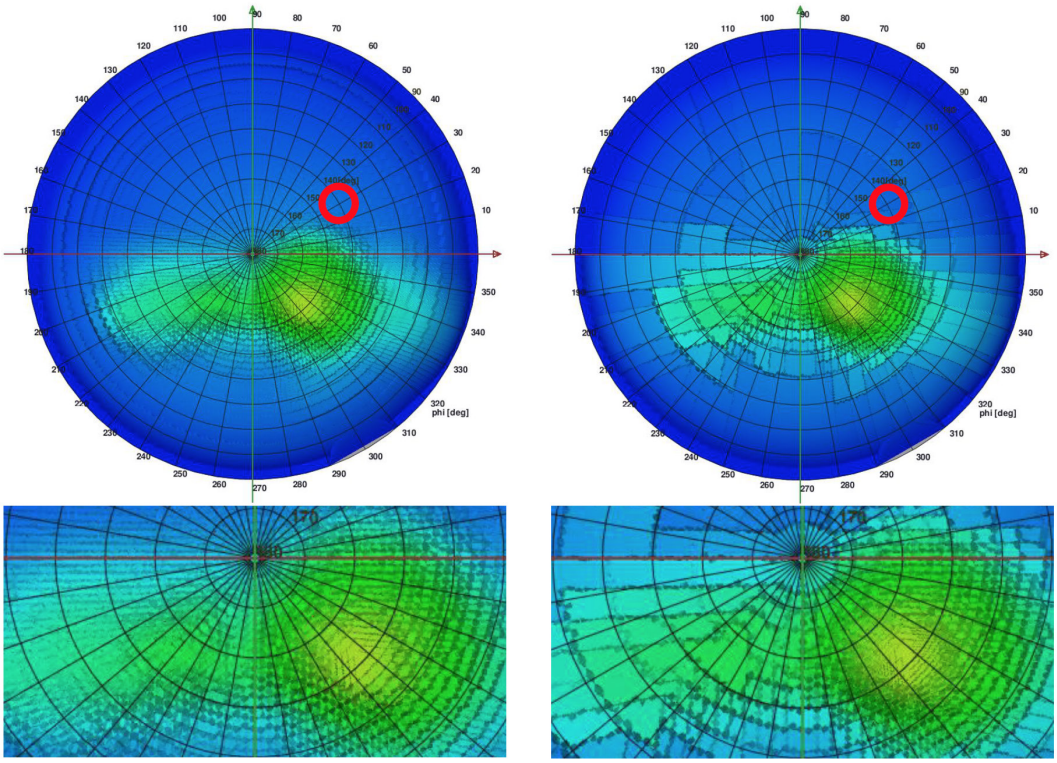

FIG. 11 DSF of DRC_1 for direction *T1* (red). Left: Resolution k=6, no data-reduction. Right: k=7, data-reduction by pt=97%.

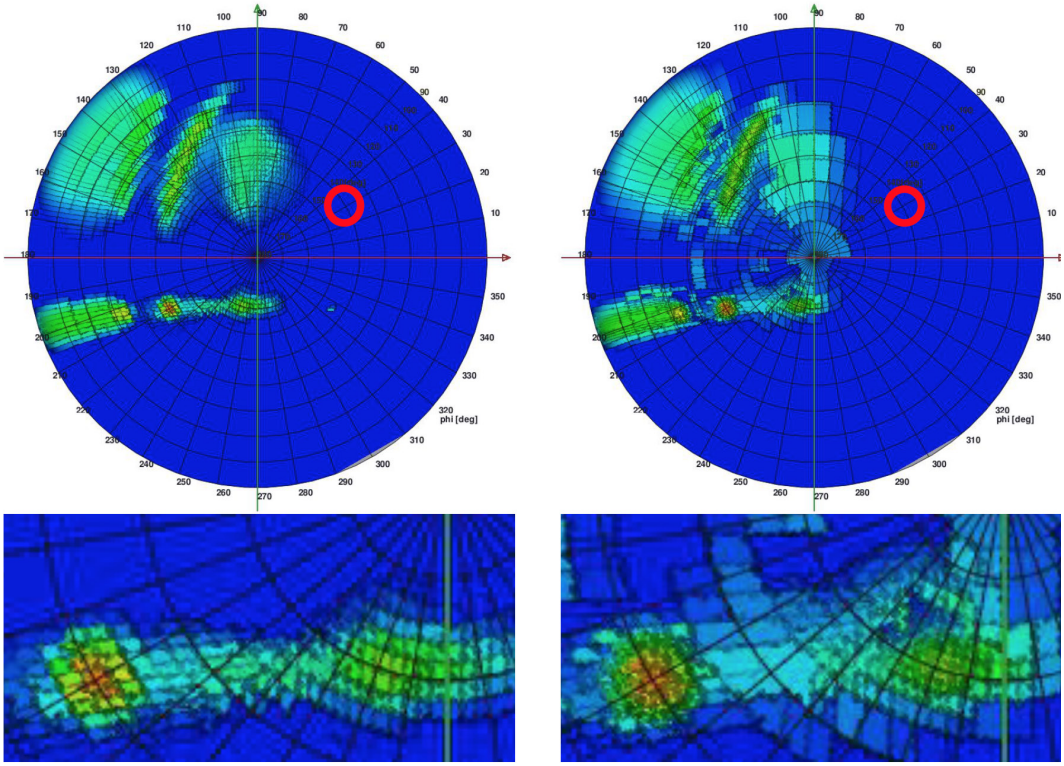

FIG. 12 DSF of DRC_2 for direction *T1* (red). Left: Resolution k=6, no data-reduction. Right: k=7, data-reduction by pt=97%.

3.5 CONCLUSIONS AND OUTLOOK

Data-driven models of two exemplary, micro-structured DRCs were generated based on measurements of their BSDF employing a gonio-photometer. The tensor-tree format of Radiance was employed, as it provides a generic means to model the irregular optical properties characterizing DRCs based on computation or measurement. Resulting models can be applied directly in daylight simulations with Radiance, or can be efficiently combined with BSDF of other clear or non-scattering fenestration layers using an extended matrix formalism. The influence of interpolation and extrapolation, depending on the density of measurements as input for the model generation, was evaluated, along with the impact of model output parameters such as directional resolution and data-reduction.

While the data-driven model in Radiance is found to be capable of modeling the irregular BSDFs of both DRC_1 and DRC_2 by interpolation, less pronounced peaks such as the downward transmission through DRC_1 may be underestimated. Resolution of measured incident directions is of particular importance for DRCs that abruptly change their properties between incident directions, such as DRC_2, if details of the complex BSDF are to be maintained.

Extrapolation for a complex BSDF, as a characteristic of DRC, was not reliable, and did not lead to valid results for either of the assessed samples. Consequently, models must be utilized only within the boundaries of measurements employed in model generation. Computational simulation to complement measurements even up to grazing have been demonstrated (Krehe, l) but require detailed prior knowledge about the geometry and surface properties of DRCs. The extension of the geometrical boundaries to higher incident elevation angles poses a challenge. The sampling aperture illuminated by a beam of circular diameter chosen to cover a representative amount of periodical

features of a given DRC at normal incident tends to exceed the sample size at high elevation angles. While this can be addressed, for example by shaping the beam employing elliptical or slit baffles, the resulting loss of beam power affects the signal to noise ratio of the measurement.

Data-reduction merges contiguous directions of low variance. This allows locally high resolution, e.g. of distinct peaks at comparable file sizes, but effects less pronounced features such as ridges in the BSDF of DRC_2.

The sensitivity of model accuracy to directional resolution and data-reduction depends on the complexity of the BSDF, and shall be further studied for different classes of DRCs. Efficient configurations of the illuminator are currently being investigated to limit the sampling aperture to the sample size even at very high incident directions.

The tensor-tree format and the routines for interpolation of measured BSDF implemented in Radiance provide a means to model DRCs characterized by high directional selectivity and highly directional, irregular transmission. Its variable resolution promises higher accuracy in daylight simulation compared to the commonly used BSDF models of low directional resolution. In order to guide model generation and application employing the tensor-tree, a better understanding of the impact of directional resolution on assessments of different aspects of daylight performance, such as daylight supply, glare and energy-efficiency, is required.

Endnotes

1. The command line parameters for bsdf2ttree are *-t4 -g 7 -t 90* for a four-dimensional tensor of initial directional resolution 2^{4*7}. The target for the data reduction is 90%.
2. bsdf2ttree called with parameters *-t4 -g 6 -t -1*.
3. bsdf2ttree called with parameters *-t4 -g 7 -t 97*.

Acknowledgments

This research was supported by the Swiss Federal Office of Energy SFOE (#SI501427-01) as part of the project "High Resolution Complex Glazing Library (BIMSOL)". Sole responsibility for content and conclusions lies with the authors.
DRC_1 was provided by the Solar Energy and Building Physics Laboratory at École Polytechnique Fédérale de Lausanne, its BSDF measured by Marek Krehel. Siteco Beleuchtungstechnik GmbH contributed DRC_2. "The work was further supported by the doctoral funding scheme of Lucerne University of Applied Sciences and Arts."

Thanks to Carsten Bauer for providing Figure 1 and Martin Vogel for Figure 3.

References

Appelfeld, D., McNeil, A., & Svendsen, S. (2012). An hourly based performance comparison of an integrated micro-structural perforated shading screen with standard shading systems. *Energy and Buildings*, 50, 166-176.

Apian-Bennewitz, P. (2010). New scanning gonio-photometer for extended BRTF measurements. In *Proceedings SPIE*, 7792 Reflection, Scattering, and Diffraction from Surfaces II, 779200-779200-20. Brussels: International Society for Optics and Photonics.

de Boer, J. (2005). Modelling indoor illumination by CFS based on bidirectional photometric data. Technical report, International Energy Agency Task 31.

Gago, EJ., Muneer, T., Knez, M., Köster, H. (2015). Natural light controls and guides in buildings. Energy saving for electrical lighting, reduction of cooling load. *Renewable and Sustainable Energy Review*s, 41, 1–13.

Greenup, P., Edmonds, I., and Compagnon, R. (2000). Radiance algorithm to simulate laser-cut panel light-redirecting elements. *Lighting Research and Technology,* 32, 49–54.

Grobe, LO., Müllner, K., & Meyer, B. (2015). A novel data-driven BSDF model to assess the performance of a daylight redirecting ceiling panel at the Calgary Airport Expansion. In *Proceedings PLDC 5th Global Lighting Design Convention*, 240-243. Rome: VIA-Verlag.

Grobe, LO. (2017). Computational combination of the optical properties of fenestration layers at high directional resolution. *Buildings, 7*, 22.

Hoffmann, S., Lee, ES., McNeil, A., Fernandes, L., Vidanovic, D., & Thanachareonkit, A. (2016). Balancing daylight, glare, and energy-efficiency goals: An evaluation of exterior coplanar shading systems using complex fenestration modeling tools. *Energy and Buildings*, 112, 279-298.

Kazanasmaz, T., Grobe, L.O., Bauer, C., Krehel, M., & Wittkopf, S. (2016). Three approaches to optimize optical properties and size of a South-facing window for spatial Daylight Autonomy. *Building and Environment*, 102, 243-256.

Kämpf, JH. and Scartezzini, JL. (2011). Ray-tracing simulation of complex fenestration systems based on digitally processed BTDF data. In *Proceedings CISBAT 2011*, 349-354.

Klems, JH. (2013). Complex Fenestration Calculation Module. In *EnergyPlus Engineering Reference*. Ernest Orlando Lawrence Berkeley National Laboratory.

Krehel, M., Grobe, L.O., & Wittkopf, S. (2017). A hybrid data-driven BSDF model to predict light transmission trough complex fenestration systems including high incident directions. *Journal of Facade Design and Engineering*, vol 5, no 2.

Kuhn, T. E., Herkel, S., Frontini, F., Strachan, P., and Kokogiannakis, G. (2011). Solar control: A general method for modelling of solar gains through complex facades in building simulation programs. *Energy and Buildings*, 43, 19-27.

Laouadi, A. and Parekh, A. (2007). Optical models of complex fenestration systems. *Lighting Research and Technology*, 39, 123-145.

Maamari, F., Andersen, M., de Boer, J., Carroll, W. L., Dumortier, D., and Greenup, P. (2006). Experimental validation of simulation methods for bi-directional transmission properties at the daylighting performance level. *Energy and Buildings*, 38, 878-889.

McNeil, A. and Lee, E. (2013). A validation of the Radiance three-phase simulation method for modelling annual daylight performance of optically complex fenestration systems. *Journal of Building Performance Simulation*, 6, 24-37.

McNeil, A., Lee, ES., and Jonsson, JC. (2017). Daylight performance of a mi- crostructured prismatic window film in deep open plan offices. *Building and Environment*, 113, 280–297.

Mohanty, L., Yang, X., and Wittkopf, S. (2012). Optical scatter measurement and analysis of innovative daylight scattering materials. *Solar Energy*, 86, 505-519.

Nair, MG., Ramamurthy, K., and Ganesan, AR. (2014). Classification of indoor daylight enhancement systems. *Lighting Research and Technology*, 46, 245–267.

Noback, A., Grobe, LO., and Wittkopf, S. (2016). Accordance of light scattering from design and de-facto variants of a daylight redirecting component. *Buildings*, 6, 30.

Ruck, N., Aschehoug, Ø., Aydinli, S., Christoffersen, J., Courret, G., Edmonds, I., Jakobiak, R., Kischkoweit-Lopin, M., Klinger, M., Lee, E., Michel, L., Scartezzini, JL., and Selkowitz, S. (2000). Daylight in Buildings - A source-book on daylighting systems and components. Lawrence Berkeley National Laboratory.

Schregle, R., Bauer, C., Grobe, LO., and Wittkopf, S. (2015). EvalDRC: A tool for annual characterisation of daylight redirecting components with photon mapping. In *Proceedings CISBAT 2015 Future Buildings and Districts Sustainability from Nano to Urban Scale*, 217-222.

Schregle, R., Grobe, LO., and Wittkopf, S. (2016). An out-of-core photon mapping approach to daylight coefficients. *Journal of Building Performance Simulation*, 9, 620-632.

Ward, G. and Shakespeare, R. (1998). Rendering with Radiance. Morgan Kaufmann Publishers, 579-580.

Ward, G., Mistrick, R., Lee, E., McNeil, A., and Jonsson, J. (2011). Simulating the daylight performance of complex fenestration systems using bidirectional scattering distribution functions within Radiance. *Leukos*, 7, 241-261.

Ward, G., Kurt, M., & Bonneel, N. (2012). A practical framework for sharing and rendering real-world bidirectional scattering distribution functions. Technical report, Lawrence Berkeley National Laboratory.